JOURNAL OF AIRCRAFT
Vol. 48, No. 1, January–February 2011

Optimal, Environmentally Friendly Departure Procedures for Civil Aircraft

R. Torres* and J. Chaptal†
Airbus, S.A.S., 31060 Toulouse, France
and
C. Bès‡ and J.-B. Hiriart-Urruty§
Université de Toulouse, 31077 Toulouse, France

DOI: 10.2514/1.C031012

In the current aviation context, one of the major concerns of commercial aviation stakeholders is to improve the environmental footprint of aviation. This research, integrated into the European Clean Sky project, addresses the optimization of commercial aircraft departure procedures in order to minimize their environmental footprint. The environmental impact is defined by noise nuisance in the protected zones near airports, local air quality, and global warming. A recent, innovating method is proposed to solve the problem of a real-world aircraft departing from an ideal airport. A multiobjective, constrained, nonlinear optimization problem is formulated to obtain optimal departure procedures. The promising results obtained by the application of this methodology to a theoretical but representative scenario strongly encourage research activities in this direction.

Nomenclature

C_I	=	cost index
$N1_{\text{noise}}$	=	intermediate, constant engine rating during a noise abatement departure procedure
V_{noise}	=	intermediate speed during a noise abatement departure procedure
V_{ZF}	=	zero flaps speed
Z_{pa}	=	acceleration altitude
Z_{pf}	=	final altitude of a noise abatement departure procedure
Z_{pr}	=	thrust-cutback altitude of a noise abatement departure procedure
ΔV_2	=	speed increment on $V2$ for initial acceleration of noise abatement departure procedure

I. Introduction

COMMERCIAL aviation has been in constant evolution since the origin of air transportation. Some of the past challenges were to improve flight safety, passenger comfort, aircraft engine and aerodynamic efficiency, aircraft flyability, structural aircraft weight, and fleet management aspects. However, progressive urban expansion, increasing air traffic growth, and recent research on climate change have led to new challenges to reduce the environmental impact. In this context, the Advisory Council of Aviation for Research in Europe's environmental research targets for 2020 are to cut carbon dioxide emissions by 50%, reduce NOx emissions by 80%, and reduce perceived noise to one half of the 2000 average levels [1]. These targets can only be achieved through a collaborative effort by all commercial aviation stakeholders: engine manufacturers to develop more efficient powerplant systems, aircraft manufacturers to improve aircraft weight and aerodynamic efficiency, and air traffic management (ATM) authorities to implement a new organization of the air space for sustainable air traffic growth while keeping the environmental footprint of aviation in mind.

The aim of this paper is to develop a methodology for reducing the environmental footprint of current in-production aircraft by optimizing aircraft departure procedures. As such, this paper is an illustration of one promising way to achieve a better environmental footprint through operations. According to the International Civil Aviation Organization (ICAO) [2], the environmental impact of aviation is defined by the effect of perceived noise on the ground, local air quality, and global warming. Departure procedures are one major area that deserves interest, because they affect perceived noise and local air quality directly and global warming indirectly.

The certification process of aircraft noise relies on sound technical-based assumptions, and it aims at guaranteeing progress toward more aircraft noise-efficient designs. As such, the certified noise levels do not totally reflect the noise produced by the aircraft during everyday operations. The minimization of noise nuisances around airports strongly depends on the location of the protected zone; therefore, noise nuisance optimization can only be performed on a targeted area. Then, to reduce noise pollution due to aircraft departure operations around airports, the ICAO proposes two general families of procedures: the noise abatement departure procedure (NADP) 1 and the NADP 2 flight-path patterns. These general procedures involve a power reduction before setting a climb rating. In the NADP 1, thrust cutback occurs before starting the acceleration and flaps/slat retraction that leads the aircraft to the clean configuration that permits the beginning of the climb phase. This procedure is specially recommended to reduce perceived noise in zones close to the airport. In contrast, the sequence is inverted in NADP 2 to reduce noise nuisances in zones located further away the airport [3]. However, to obtain significant environmental improvements, these general recommendations must be adapted to each specific aircraft and airport [4–9].

Local air quality can be described as the condition of the ambient air to which human beings and nature are typically exposed. Commonly accepted methods determine air quality by assessing the concentration of pollutants [10,11]. One of the pollutants generated by aircraft engines affecting local air quality is nitrogen oxides (NOx). These are emitted in the flight segments taking place in the low troposphere, departure and approach/landing segments. Nevertheless, engines are operated at low-power levels during approach and landing phases, power levels for which emissions of NOx are

Received 9 March 2010; revision received 8 June 2010; accepted for publication 9 June 2010.

*Research Engineer and Ph.D. Candidate, On-Board Systems Department, Boîte Postale M01/31, 316 Route de Bayonne, Cedex 09. Member AIAA.
†Airbus Engineer, On-Board Systems Department, Boite Postale M01/31, 316 Route de Bayonne, Cedex 09.
‡Professor, Mechanical Engineering Department, 118 Route de Narbonne, Cedex 4. Member AIAA.
§Professor, Applied Mathematics Department, 118 Route de Narbonne, Cedex 4.

low, and the concentration of NOx is thus mainly affected by the departure.

There is a scientific consensus on the fact that the contribution of aviation to global warming mainly concerns the production of carbon dioxides (CO_2). Nitrogen oxides generated in the upper troposphere also contribute to global warming through the formation of tropospheric ozone, but NOx also contributes to the reduction of methane, which is a positive effect [12]. So, its overall contribution to global warming can be neglected, and only CO_2 emissions are considered. The scientific community estimates that aviation generates around 3% of the overall carbon dioxide production and 13% of the carbon dioxides due to transportation [13–15]. Because of the continuous growth of air traffic [16,17], the scientific community states this contribution may increase significantly in the future. Focusing on the aviation sector and how aircraft are operated on one single mission, carbon dioxide effects are not altitude dependent; therefore, the impact of CO_2 emissions is similar along the whole flight path. This means that the most important improvement on the effect on global warming can be obtained by optimizing the climb, cruise, and descent segments, which cover most of the aircraft mission. The ambitious target to include global warming in a concept of departure procedure optimization could be surprising, but it is justified by the fact that the departure procedure will influence the rest of the flight path, involving an indirect effect on global warming.

The study involved in this paper, integrated into the European Clean Sky Joint Technology Initiative project, deals with the alleviation of the environmental impact of a single in-production aircraft by optimizing the departure procedure. The next four sections of this paper focus on the framework and formulation of this environmental, multicriteria optimization concept. Section II introduces the general characteristics of the three environmental criteria: perceived noise on ground, engine emissions of nitrogen oxides, and carbon dioxides. Section III describes the general pattern of the departure procedure to be optimized and its computation principles. Departure procedure constraints are presented in Sec. IV. Then, Sec. V presents a recent and efficient algorithm for solving this multiobjective optimization problem (MOOP). Section VI presents an example of a current in-production aircraft departing from an ideal airport. The methodology is illustrated using aircraft data provided by Airbus Operations, S.A.S. To avoid a computational burden and favor physical understanding of the optimization results, the three environmental criteria are initially optimized by pairs. For this application, the optimal solutions of the scenarios are described in terms of environmental gains and flight-path variables. Finally, in Sec. VII, conclusions and further open perspectives are presented.

II. Optimization Criteria

A. Perceived Noise on the Ground

The noise perceived on the ground is estimated through the Airbus Noise Level Calculation Program (NLC), the Airbus software delivered to airlines to predict operational noise [18]. The NLC uses a database dedicated to each aircraft model (airframe/engine combination) to compute the overall generated noise as a punctual source to which flight effects, atmospheric propagation, and ground effects are applied. This database, derived from static engine noise tests and Airbus airframe noise models, contains total aircraft noise spectra depending on speed, aerodynamic configuration, and engine rating. Note that NLC takes the aircraft operational trajectory data as input.

In practical applications, the noise criterion may be different for each departing airport. The formulation and resolution of the problem developed in this paper can consider any noise criterion involving a single departure (average perceived noise, maximum level, etc.). However, any single-event noise metrics can be used, from perceived noise metrics to maximum noise levels (effective perceived noise level, A-sound exposure level, sound exposure level, tone perceived noise level, etc.).

B. Local Air Quality

Aircraft engine emissions throughout the flight path can be computed using a fuel flow correlation [19]. In this correlation; NOx emissions are computed through a temporal integration along the flight path of the product of a factor specific to each pollutant, called the emission index (EI), and engine fuel flow [19]. In the case of nitrogen oxides, the emission index $\mathrm{EI}_{\mathrm{NOx}}$ depends on the atmospheric conditions (pressure, temperature, and humidity), the aircraft speed, and the engine fuel flow. Nitrogen oxides are harmful for air quality in the lower troposphere. The border altitude that limits the impacted zone (threshold altitude) depends on the airport location and atmospheric conditions. International organizations typically set the threshold altitude $h_{\mathrm{threshold}}$ at 3000 ft above ground level (AGL) [11]. Following this model, NOx emissions can be computed using Eq. (1):

$$\mathrm{NOx} = \int_{h=0}^{h_{\mathrm{threshold}}} (\mathrm{EI}_{\mathrm{NOx}}\,\mathrm{fuelflow})\,\mathrm{d}t \tag{1}$$

The evolution of the emission index during the studied flight segment is secondary compared with the evolution of fuel flow. So, in an initial approach, minimizing air quality impact can be equivalent to minimizing the fuel burn at low altitudes.

C. Global Warming

The impact of carbon dioxide emission is similar along the flight path and is thus related to the total amount of CO_2 emissions. Also, since CO_2 is a direct combustion product (unlike NOx, which is a pollutant linked to the imperfection of the combustion), CO_2 emissions are directly related to the composition of the fuel. This study considers current fuels, which are approved for use in the aviation sector, excluding alternative fuels. The carbon dioxide emission index $\mathrm{EI}_{\mathrm{CO2}}$ is therefore considered constant (typically 3.15 kg CO_2/kg fuel). As a consequence, minimizing carbon dioxide emissions is equivalent to minimizing fuel burn. On an operational point of view, the minimization of fuel burn can be included in the optimization of the direct operating cost (DOC), which includes the costs associated with the flight duration $\boldsymbol{\Delta T}$ and fuel burn $\boldsymbol{\Delta F}$. The emissions of CO_2 are included in the study by adding the cost of 1 kg of carbon dioxide $\boldsymbol{C}_{\mathrm{CO2}}$ to the cost of 1 kg of fuel burn $\boldsymbol{C_F}$. Airlines use the concept of cost index $\boldsymbol{C_I}$ to balance the costs of fuel versus the costs of time $\boldsymbol{C_T}$. The cost index corresponds to the time and fuel costs ratio [20]. In other words, the cost index permits the defining of the equivalence of time costs in fuel costs; therefore, the DOC can be measured in equivalent fuel units:

$$\mathrm{DOC} = \boldsymbol{C_F}\left[1 + \frac{\mathrm{EI}_{\mathrm{CO2}}\boldsymbol{C}_{\mathrm{CO2}}}{\boldsymbol{C_F}}\right]\boldsymbol{\Delta F} + \boldsymbol{C_T}\boldsymbol{\Delta T} \tag{2}$$

The problem can be transformed to the standard formulation by defining an environmental cost index $\boldsymbol{C}_{I,\mathrm{ENV}}$ similar to the standard definition but using an extended fuel cost that includes carbon dioxide costs. To adapt Eq. (2) to the current formulation, the optimization criterion for the DOC is divided by the sum of fuel burn and CO_2 emission costs:

$$\overline{\mathrm{DOC}} = \boldsymbol{\Delta F} + \boldsymbol{C}_{I,\mathrm{ENV}}\boldsymbol{\Delta T} \tag{3}$$

Formulation of Eq. (3) enables the solving of the optimization of global warming by using the existing cost index optimization methodologies. The equivalence between both problems is based on readjusting the standard cost index value in order to take into account the optimization of carbon dioxides.

The global warming criterion is the $\overline{\mathrm{DOC}}$ measured at a common mission point, which is defined by a certain aircraft speed, altitude, aerodynamic configuration, and distance covered, and assuming standard weather conditions. It is worth noting that, in the case of $C_I = 0$, this is the main difference between the air quality and the CO_2 criteria. Broadly speaking, while an air quality criterion aims to minimize fuel burn under the threshold altitude, a CO_2 criterion will aim to minimize fuel burn up to the common mission point. For the sake of clarity, the common mission point is usually located in the cruise phase. Note that the climb and cruise phases are fixed for all the

departure procedures simulated in this study. For simplicity, the global warming criterion $\overline{\text{DOC}}$ is simply denoted as DOC.

III. Departure Procedures

The departure procedure can be separated into two different segments. The takeoff distance corresponds to the aircraft takeoff path from the brake release point up to an altitude of 35 ft AGL. This segment is strongly constrained to guarantee safety conditions, so it is not optimized in this study. The optimization problem deals with the takeoff flight path, which is the flight phase that links the initial segment to the climb phase. Note that, in real operating conditions, aircraft lateral routes are constrained to the procedures published at the departure airport, so optimization will only concern vertical guidance (e.g., altitude and speed).

The takeoff flight path is modeled through an enhanced NADP (E-NADP) pattern, which is an extended version of the NADP 1 and NADP 2 patterns. While NADP 1 and NADP 2 patterns start at 800 ft, the E-NADPs proposed in this study start at 35 ft. Moreover, an intermediate speed before reaching the climb speed, usually 250 kt, can also be optimized. The NADPs were originally designed to reduce the perceived noise on ground but, in this study, the variables describing this pattern are optimized to also improve the other two environmental criteria. The obtained departure procedures must be easy to implement, so they are described through a small number of segments that are defined through six variables. These procedures propose the addition of intermediate segments between 35 ft and the en route configuration point at which the aircraft is operated with specific speed and reduced engine rating. This segment-based approach is described in detail in this section: the beginning and end of the optimized flight phase and the evolution of the aircraft speed and thrust during the segment-based approach.

The E-NADPs begin once the rollout phase has finished, at an altitude of 35 ft AGL. Although the aircraft settings at takeoff are not optimized, they will have an important influence on the departure procedure. Takeoff performance (flap setting, speeds, and takeoff thrust) is established based upon certified limitations published in the aircraft flight manual. These initial conditions are computed using takeoff and landing optimization with the Airbus certified software used during the flight preparation to compute the takeoff performance variables for the day conditions [18]. Accordingly, the complete set of safety constraints is strictly adhered to.

The E-NADPs finish at the en route configuration point, where the climb phase starts. This state is defined by a prescribed aircraft speed and flight level, which are common to all the departure procedures simulated in this study. Figure 1 illustrates the flight phases up to the common mission point and the main environmental concern affected on each phase.

The three environmental criteria are optimized through six optimization variables that characterize the E-NADP, described next. The overall departure procedure can be represented in speed-altitude and engine rating-altitude diagrams, as shown in Fig. 2. Speed laws are managed in terms of calibrated air speed (CAS).

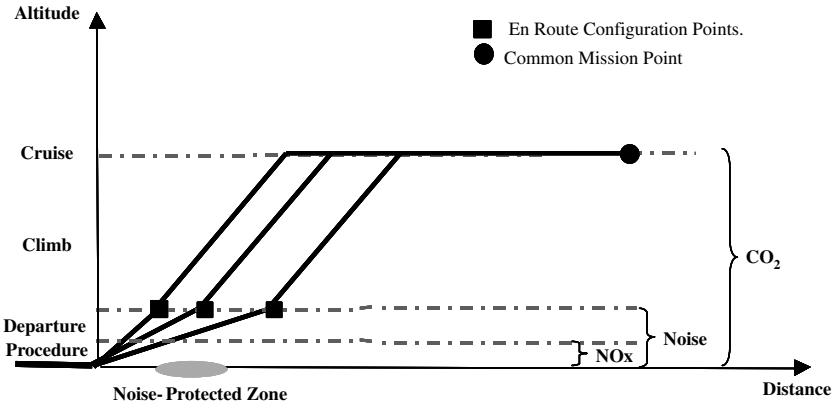

Fig. 1 Aircraft environmental footprint at low altitudes.

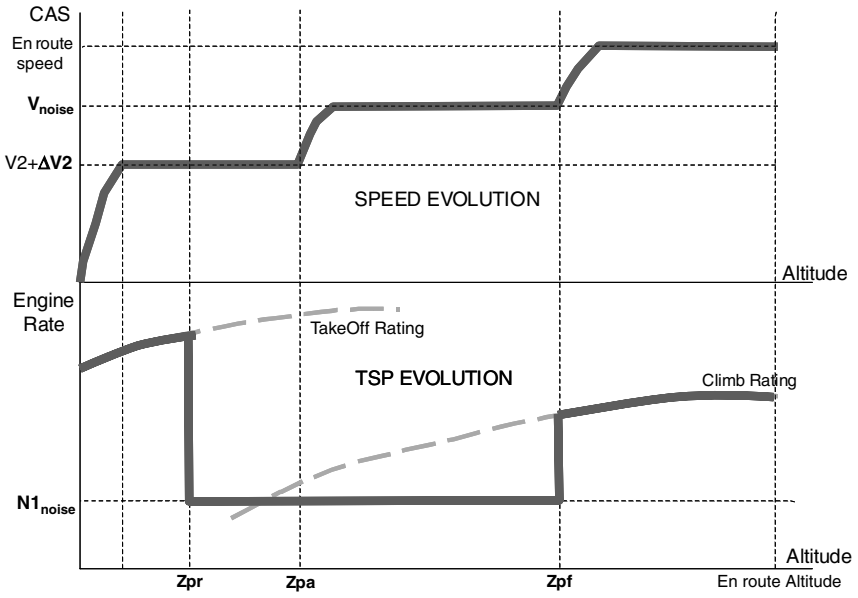

Fig. 2 Flight-path variables.

The aircraft speed evolution during the E-NADP is defined through four optimization variables that define three acceleration segments. The first acceleration starts at 35 ft and finishes at a target speed defined as the addition of the regulatory speed V_2 and the optimization variable ΔV_2 (instead of the currently used V_2+ 10 kt). The second acceleration segment is characterized by two optimization variables: the altitude at which the acceleration starts Z_{pa} and the target speed V_{noise}. Flaps and slats are retracted during this acceleration, so at the end of this segment, the aircraft is at a clean configuration. The final acceleration leads the aircraft to the en route speed. So, the only possible optimization variable is the altitude at which the acceleration starts: the so-called final noise altitude Z_{pf}.

The thrust evolution is defined through the engine rate profile, which is characterized by three variables. As mentioned before, the takeoff engine rating is defined by other criteria and not environmentally based. Once the cutback altitude Z_{pr} is reached, the engine rate is reduced to a fixed thrust setting parameter (TSP) named $N1_{\text{noise}}$. Finally, thrust is restored to the climb rate at Z_{pf}.

In summary, the departure procedure can be parameterized through two sets of variables: one to describe the evolution of the aircraft speed $(\Delta V_2, Z_{pa}, V_{\text{noise}}, Z_{pf})$ and another to describe evolution of the thrust $(Z_{pr}, N1_{\text{noise}}, Z_{pf})$. The two sets of variables are coupled through the variable Z_{pf}.

This segment-based approach may have some limitations. For instance, the E-NADP concept could be extended to include multiple thrust-cutback maneuvers or optimized acceleration laws (e.g., constant rate of climb, energy sharing law, and prescribed rate of climb). Nevertheless, this first research relies on current system design and capacities.

To obtain realistic results, the flight path is calculated using the operational flight-path software (OFP) provided by Airbus to airlines to compute the operational flight paths in the neighborhood of airports [18]. In this software, the vertical profile is described by a set of discrete segments. The general flight mechanics equations are solved at each segment using aircraft-specific databases for the current flight conditions. These databases contain realistic models of the aircraft configuration (geometry, landing gear, load distribution, braking, aerodynamics, engines, and characteristic speeds) and the atmospheric conditions. Computing the departure procedures with OFP permits an accurate flight-path definition by describing each and every discrete event that occurs in this flight segment, such as landing gear retraction or a change of the aerodynamic configuration to be modeled. This means that computation of the aircraft trajectory is a nonlinear discontinuous function. In this study, OFP is considered as a black box. For given initial conditions, OFP takes the six E-NADP variables as input and provides the aircraft trajectory as output.

IV. Constraints

The complexity of the problem is increased by the presence of a high number of constraints in the departure procedure. Operational constraints during the departure procedures concern the feasibility, safety, and comfort of the proposed procedures. Aircraft performance limitations (e.g., maximum attitude, maximum load factor, maximum allowed speeds for each configuration, etc.), specific safety conditions to NADPs (e.g., initialization conditions of the procedure, minimum engine rating to assure a minimum path angle when one engine fails, etc.), or en route constraints concerning obstacle clearance are some of these constraints. Table 1 shows the main operational constraints considered in this study and the application domain.

The upper and lower bounds of the optimization variables are based on the ICAO recommendations for NADP 1 and NADP 2 and ATM constraints. For these procedures, the acceleration and thrust-cutback altitudes, Z_{pa} and Z_{pr}, must be higher than 800 ft and lower than 3000 ft AGL. However, the final altitude Z_{pf} can take higher values (only limited by 10,000 ft). Similarly, the initial acceleration must be between $V_2 + 10$ and $V_2 + 20$ kt. The target speed V_{noise} is limited by the fact that, during the departure procedure, the aircraft must not decelerate, so it must be higher than $V_2 + \Delta V_2$. Moreover, flaps and slats must be retracted in the acceleration after Z_{pa}, so V_{noise} must be higher than the V_{ZF} speed (zero flaps speed). Finally, general ATM constraints limit the aircraft speed to 250 kt for altitudes under 10,000 ft. As shown in Table 1, additional restrictions are considered in the case of NADP 2.

Table 1 Main operational constraints

Constraint	Domain
Obstacle clearance	Whole flight path
Start of the procedure with landing gear retracted	Departure procedure
Maximum pitch angle	Whole flight path
Maximum speed for each aerodynamic configuration	Whole flight path
No deceleration permitted	Departure procedure
Acceleration target speed limited by V_{ZF}	Departure procedure, in case $Z_{pa} < Z_{pr}$
Bound constraints	Departure procedure
ATM constraints	Departure procedure

Also, in this study, thrust cutback $N1_{\text{noise}}$ is bounded by the climb engine rating and a positive angle of climb in case of engine failure while flying at thrust cutback.

Another type of constraint comes from the ATM regulations around each particular airport. These constraints usually gather variables from the vertical profile and the lateral route. For instance, the angle of climb or aircraft speeds (vertical profile variables) are limited up to prescribed waypoints defined in the aircraft lateral route.

The last constraints concern the resolution of the optimization problem. The variables defining the flight path must be combined in such a way that they have a physical sense. For example, segments at a reduced rating must occur before setting the climb rating.

All these restrictions generate a set of up to 20 constraint functions. All these constraints can be represented through a set of nonlinear mathematical functions that have to satisfy inequality conditions:

$$\boldsymbol{G}(\boldsymbol{x}) \leq 0, \qquad \boldsymbol{x} \in \Re^6, \quad \text{and} \quad \boldsymbol{G} \in \Re^{\boldsymbol{l}} \tag{4}$$

where $\boldsymbol{G}$ is the set of constraint functions, $\boldsymbol{l}$ is the number of constraints ($\boldsymbol{l} \approx 20$), and $\boldsymbol{x}$ is the vector of six optimization variables.

V. Optimization Algorithm

Three criteria (perceived noise on the ground, the production of nitrogen oxides, and DOC) must be optimized through six constrained variables that model the departure procedure.

In the general solution of a MOOP, it is not possible to determine a single optimal solution, but it is possible to determine a set of optimal solutions. In this research, optimum solutions are defined using the notion of Pareto optimality. A feasible solution is called efficient or Pareto optimal if any improvement in one of the criterion necessarily involves deterioration in the other criteria. Efficient solutions are also named nondominated points [21].

The general formulation of a multiobjective constrained optimization problem is presented in Eq. (5):

$$\text{MOOP}: \min_x F(x) = [f_1(x), f_2(x), \ldots\ldots, f_n(x)] \tag{5}$$

subject to

$$G(x) \leq 0$$

where the objective function $\boldsymbol{F}$ is composed of the different objectives $\boldsymbol{f}_i$, $\boldsymbol{n}$ is the number of objective functions to optimize, $\boldsymbol{x}$ is the vector of optimization variables, and $\boldsymbol{G}$ represents the constraints to be satisfied.

Because of specific actions during the flight path and database interpolation, objectives and constraint functions are not derivable. So it is preferable to use optimization algorithms that do not need any gradient information to find the optimum solutions. In this study, the innovating multiobjective mesh adaptive direct search

(multi-MADS) method is proposed to obtain the Pareto-optimal trajectories. This algorithm relies on the recent mesh adaptive direct search (MADS) [22,23], which has been seen to be well adapted to accomplish mono-objective, nonlinear, constrained simulation-based optimization problems. A complete description of multi-MADS can be found in [24]. In this paper, only the main algorithmic aspects are described. Based on the current dominating points, this algorithm formulates a different single-objective problem formulation (SOP) at each iteration. Dominating points obtained during the resolution of each one of these mono-objective optimization problems constitute an approximation of the Pareto front. Furthermore, this approximation of the Pareto front can be nonconvex or disjoint. The single-objective formulation SOP can be formulated as follows:

$$\text{SOP: } \min \Psi(x) = \phi[F(x)] = \phi[f_1(x), f_2(x), \ldots, f_n(x)] \quad (6)$$

subject to

$$G(x) \leq 0$$

where $\boldsymbol{\Psi}(\boldsymbol{x})$ is the single-objective distance criterion, as shown in Eq. (7). This distance criterion can be based on any norm:

$$\boldsymbol{\Psi}(\boldsymbol{x}) = \phi[\boldsymbol{F}(\boldsymbol{x})] = \begin{cases} -\text{dist}^2[\partial \boldsymbol{D}, \boldsymbol{F}(\boldsymbol{x})] & \text{if } \boldsymbol{F}(\boldsymbol{x}) \in \boldsymbol{D} \\ \text{dist}^2[\partial \boldsymbol{D}, \boldsymbol{F}(\boldsymbol{x})] & \text{otherwise} \end{cases} \quad (7)$$

where $\text{dist}[\partial \boldsymbol{D}, \boldsymbol{F}(\boldsymbol{x})]$ denotes the distance from the boundary of the current dominance zone $\boldsymbol{D}$ to $\boldsymbol{F}(\boldsymbol{x})$. The dominance zone, which is an approximation of the Pareto front, is improved at each iteration by updating the set of dominating points. Although this SOP could be solved using any of the mono-objective optimization techniques, multi-MADS uses the MADS. The multicriteria optimization process can be summarized using Fig. 3:

The efficiency of multi-MADS is mainly due to the performance of the mono-objective optimization algorithm MADS. MADS is included among the direct search methods [25]. These methods are of interest in optimization problems where the number of evaluations of the objective functions is restricted and the derivative information of the objective function either cannot be obtained or is not reliable, which is the case of the problem of obtaining clean optimal departure procedures. Pattern search methods aim to find the local optimum of the problem using a certain set of predefined directions, which do not depend on the objective function gradient. Compared with the general pattern search methods (GPS), the main innovation of MADS is the use of a set of infinite directions to span the space of variables. This technique improves the performance of the method in the presence of local optima, enhancing global optimum solutions. Moreover, in the MADS method, constraints are handled by a progressive barrier function, so no penalties are used. This methodology permits the withholding of the best feasible incumbent and it permits the best infeasible incumbent to achieve the optimum solution, which can be useful when the optimum solutions are placed in highly constrained areas [26]. Therefore, MADS seems to be particularly well adapted for obtaining the optimal, environmentally friendly departure procedures.

In MADS, each iteration is divided into two steps. The first step, called SEARCH, corresponds to a global search to determine the best current, feasible incumbent. The best incumbent must lie on a prescribed mesh, which is never explicitly calculated. This step is optional, and it is not used in the demonstration of the convergence of the algorithm. The POLL step consists of a local search around the best incumbent. Improvements from GPS algorithms rely on this step. Not only can the size of the prescribed mesh be controlled but also the size of the zone where the local search occurs, called a frame. The different MADS steps are synthesized in Fig. 4.

INITIALIZATION:
Provide an initial solution.
MAIN MADS ITERATION:
SEARCH step (optional): global search for the best current incumbent.
If search step fails,
POLL step: local search around the best incumbent.
UPDATE PARAMETERS
If POLL step succeeds, increase poll and mesh sizes (increase frame).
If POLL step fails, decrease poll and mesh sizes.
Update the progressive barrier function.

Fig. 4 MADS algorithm.

VI. Application of Environmentally Optimal Departure Procedures

In this section, the methodology is illustrated with the example of a representative aircraft departing from an ideal airport. The concept of an ideal airport was aimed at having a departure scenario that does not add any additional performance constraints, such as obstacles or runway lengths, or ATM constraints.

In the current studies, it has been stated that it is not possible to minimize noise nuisances over all the zones around the airports with a single set of flight-path parameters. This means that aircraft paths minimizing noise in zones near the airport will not guarantee noise nuisance reduction in further zones. Then, to test the efficiency of the concept, two scenarios are studied. Both have similar characteristics; they only differ in the position of the noise-protected zones. In scenario A, noise is estimated close to the airport, while in scenario B, noise is estimated further away in the distant zone. The noise optimization criterion is an arbitrary indicator of noise nuisances on each zone. Any noise optimization criterion could have been considered, such as maximum perceived noise or the average of the maximum noise level of each estimation point. In this research, to be representative of estimations of noise nuisances without penalizing computational costs, each protected zone is defined by three estimation points placed under the aircraft track. The estimation points are placed at 5.5, 6.5, and 7.5 km from the brake release point in scenario A and at 14, 15, and 16 km from the brake release to measure noise in scenario B. The noise optimization criterion is the quadratic mean value of the three noise calculations.

DOCs are measured using a commonly used value of cost index for medium-range trajectories, $C_I = 20$. The study is based upon a current in-production single-aisle aircraft. The data used for the analysis were provided by Airbus Operations, S.A.S.

Commonly used NADP 1 and NADP 2 for single-aisle aircraft, presented in [27], are considered as the baselines procedures to assess the potential environmental gains of the optimized trajectories. In the NADP 1, used as reference, the climb rating is set at 800 ft, and the accelerations toward the en route speed start at 3000 ft. On the other hand, on the baseline NADP 2, acceleration starts at 800 ft, and the climb rating is set once the clean configuration is achieved.

INITIALIZATION:
Provide an initial solution x0.
Computation of optimum solutions for each criterion: $\min_{\boldsymbol{x}} \boldsymbol{f_i}(\boldsymbol{x})$ subject to $\boldsymbol{G}(\boldsymbol{x}) \leq 0$ for $\boldsymbol{i} = 1,2,..\boldsymbol{n}$
MAIN ITERATION:
Single-objective optimization problem : ***SOP***: $\Psi(x) = \phi[f_1(x), f_2(x), \ldots f_n(x)]$
Resolution of the single objective formulation, using MADS $\min_{\boldsymbol{x}} \boldsymbol{\Psi}(\boldsymbol{x})$ subject to $\boldsymbol{G}(\boldsymbol{x}) \leq 0$
Update the set of dominating points (Pareto front).

Fig. 3 Multi-MADS algorithm.

As mentioned in the Sec. I, to avoid a computational burden and favor the physical understanding of the optimization results, the three environmental criteria are optimized in pairs. So, the specific version of multi-MADS for biobjective optimization problems (BOP), bi-MADS, [28] is used. This section is organized as follows. First, in Sec. VI.A, the Pareto-optimal fronts are presented for the four BOPs. Then, in Sec. VI.B, the potential environmental gains of optimizing the departure procedures are presented. This is done by analyzing the extreme solutions of the Pareto fronts, which correspond to the optimum levels of each criterion. Moreover, the optimal flight paths are described for each of these extreme solutions. Finally, Sec. VI.C focuses on the evolution of optimal flight paths along the Pareto fronts.

A. Environmental Pareto Fronts

In this section, the Pareto-optimal fronts obtained are presented. The NADP 1 is the departure procedure mostly used in European airports, so it is considered as the reference. Then, to justify the gains of optimizing the departure procedures, the relative environmental levels of the Pareto fronts and the NADP 2 are presented with regard to the baseline NADP 1. Figures 5 and 6 concern the noise–NOx and noise–DOC optimizations in scenario A, where noise is estimated in a zone close to the airport, and Figs. 7 and 8 represent the noise–NOx and noise–DOC optimizations when noise is optimized in the distant zones (scenario B). The DOC–NOx BOP is not represented here, because the conclusions are redundant.

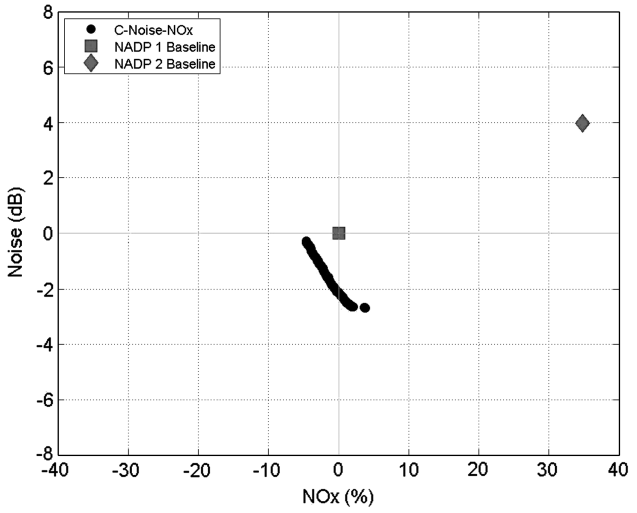

Fig. 5 BOP I: Close-in noise–NOx Pareto front.

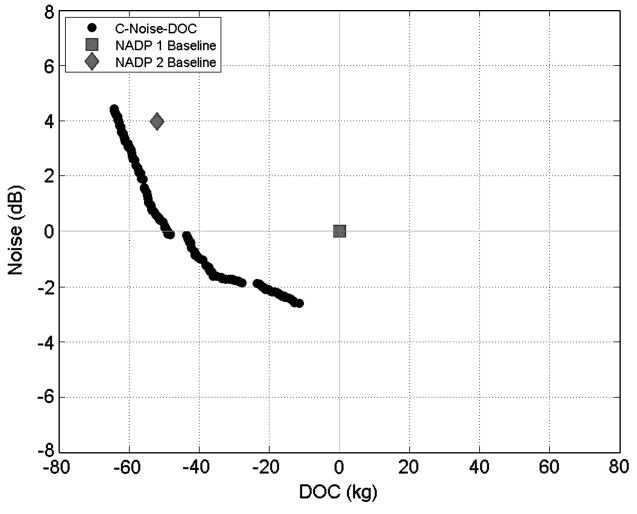

Fig. 6 BOP II: Close-in noise–DOC Pareto front.

A quick glance at the shape of the Pareto optimal detaches some discontinuities on the Pareto fronts. For reasons of clarity, these discontinuities will be justified in Sec. VI.C once the general features of the optimum paths have been described.

Each Pareto front is composed of around 500 points. The CPU time for computing each of these fronts is around 4 h on a Sun Fire 6800 with 1200 MHz CPU under a Unix Solaris 8.

B. Analysis of the Extreme Solutions of the Pareto Fronts

The aim of this section is to first assess the potential environmental gain by evaluating the extreme points of the Pareto fronts of Figs. 5–8. Second, the optimum flight paths that should be used to fulfill the minimum environmental impact levels are described.

1. Potential Environmental Gains

A quick glance at the Pareto fronts of Figs. 5–8 shows the multiobjective nature of the problem. These figures exhibit significant differences on the environmental levels of the extreme points of the Pareto fronts.

Regarding the perceived noise criteria, Figs. 5 and 6 show that E-NADP 1 paths are recommended to reduce noise in the close-in areas, whereas Figs. 7 and 8 show that E-NADP 2 paths should be used to reduce noise in zones further away from the airports. Moreover, differences in the noise perceived between the E-NADP 1 and E-NADP 2 in the close-in zone are higher than in the distant zone. Nevertheless, note that, in both cases, these reference procedures can

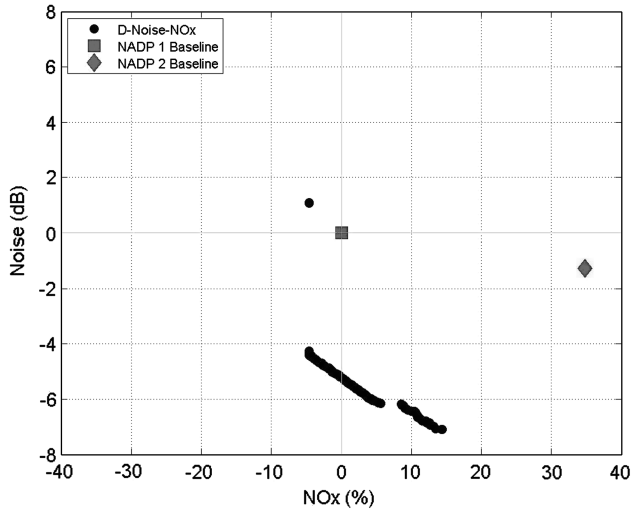

Fig. 7 BOP III: Distant noise–NOx emissions Pareto front.

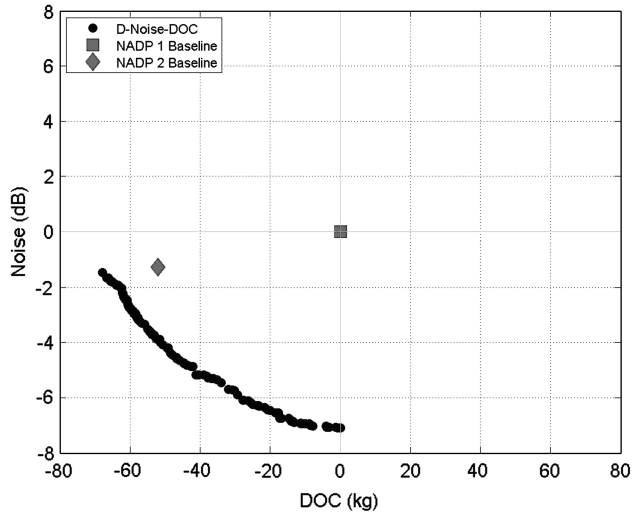

Fig. 8 BOP IV: Distant noise–DOC Pareto front.

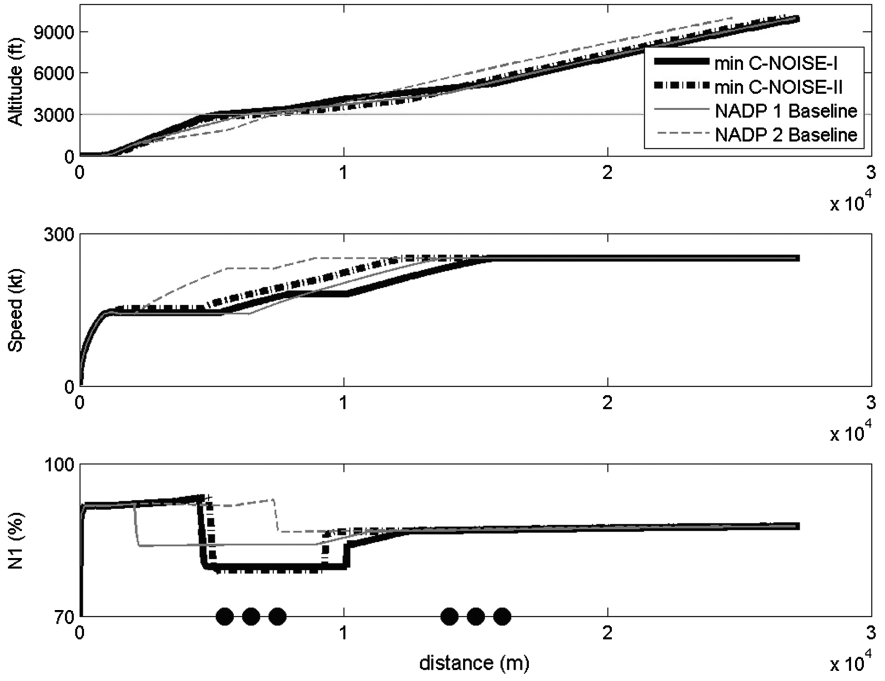

Fig. 9 Flight paths minimizing close-in noise.

be improved by using flights paths given by the proposed Pareto fronts.

The minimum level of DOC, which shall be the prior objective for the flight paths departing from airports without any air quality or noise restrictions, is close to the NADP 2 pattern type used as baseline. However, the E-NADP 2 path performs poorly with regard to the other environmental criteria. Finally, it can be seen that the quantity of NOx emitted at low altitudes while flying an E-NADP 1 trajectory type is not very far from the minimum possible NOx level.

2. *Flight Paths Minimizing the Environmental Criteria*

This section focuses on the analysis of the physical characteristics of the optimum flight paths that minimize each one of the environmental criteria. Generally, the mono-objective optimization problems of each criterion considered have multiple solutions. Among these solutions, only the one involving the minimum value of the other criterion optimized in the BOP belongs to the Pareto front. This means that the extreme points of the Pareto fronts are unique.

To be exhaustive, the two extreme points of the four optimization problems are studied. Figures 9–12 represent the altitude-, speed-, and TSP-distance diagrams associated with the extreme points of the previous Pareto fronts, classified according to the criterion they optimize. The different optimum flight-path patterns for each criterion follow the notation of Table 2 and the baseline procedures. Problems I and II correspond to the noise–DOC and noise–NOx optimizations in scenario A, while problems III and IV correspond to the same optimization problems in scenario B.

For clarity reasons, in Figs. 9–12, the boundary altitude for the NOx criterion (3000 ft) is indicated with a thin line in the upper

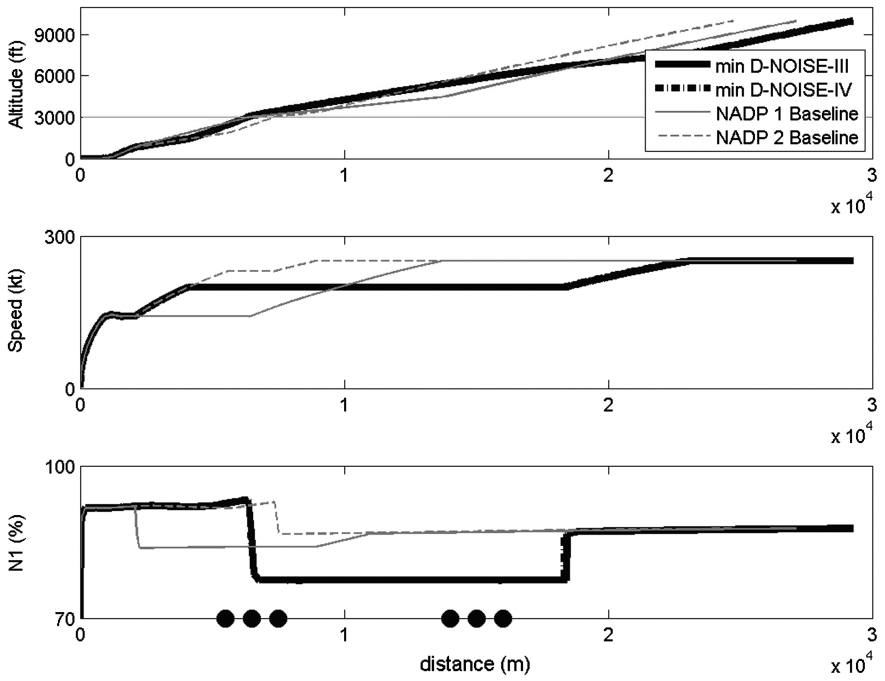

Fig. 10 Flight paths minimizing distant noise.

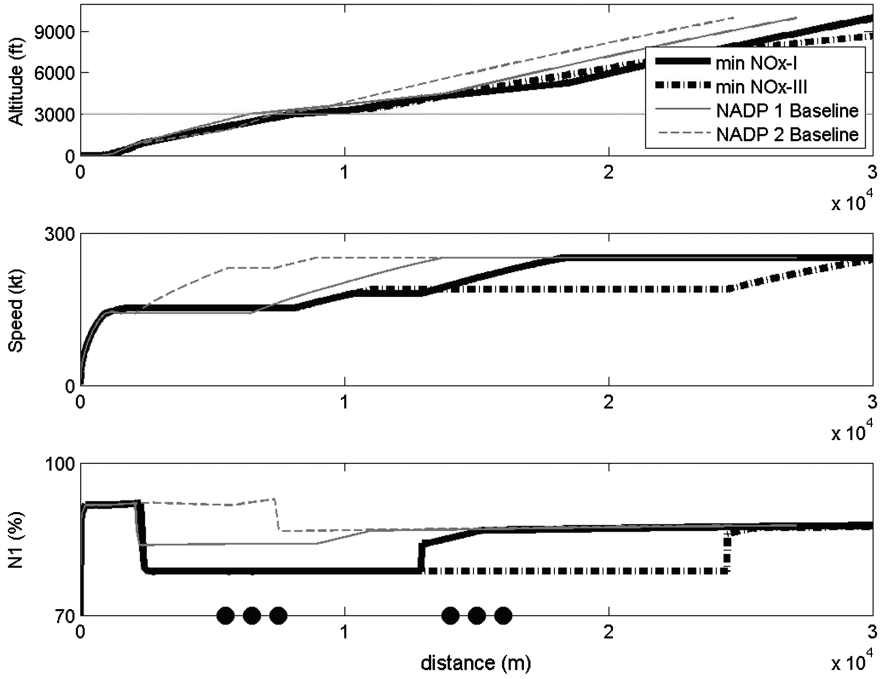

Fig. 11 Flight paths minimizing NOx.

Table 2 Optimum flight-path notation

Optimization problem	Optimal flight paths	Name
Close-in noise–NOx (I)	Min close-in noise	C-NOISE-I
	Min NOx	NOx-I
Close-in noise–DOC (II)	Min close-in noise	C-NOISE-II
	Min DOC	DOC-II
Distant noise–NOx (III)	Min distant noise	D-NOISE-III
	Min NOx	NOx-III
Distant noise–DOC (IV)	Min distant noise	D-NOISE-IV
	Min DOC	DOC-IV

subplot, and the noise estimation points are indicated with spherical marks in the bottom subplot.

The analysis first deals with the strategies to follow to minimize perceived noise on the ground in each of the selected scenarios. Second, flight paths optimizing local air quality and DOC criteria are described.

Perceived noise on the ground is optimized according to different strategies, depending on the zone where it is estimated. More precisely, for the aircraft type used in this study, perceived noise on the ground is minimized when the aircraft flies over the protected zone using a reduced engine rating at a maximum distance from the microphone. To this effect, the Pareto-optimal flight path is characterized by a thrust cutback just before flying over the noise-protected zone. For example, in close-in noise-protected areas, Fig. 9 illustrates that the aircraft does not accelerate until it has flown over

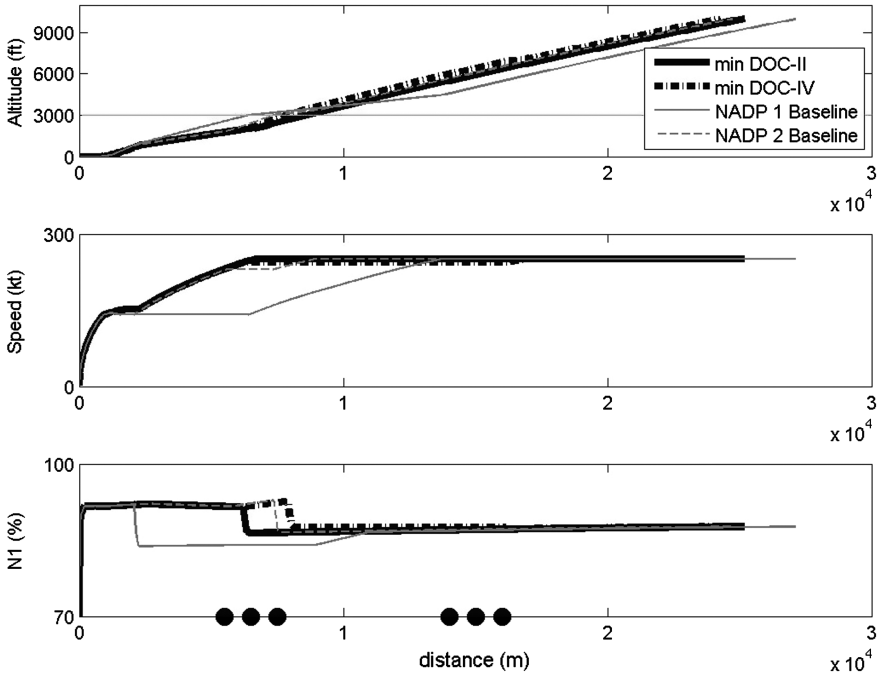

Fig. 12 Flight paths minimizing DOC.

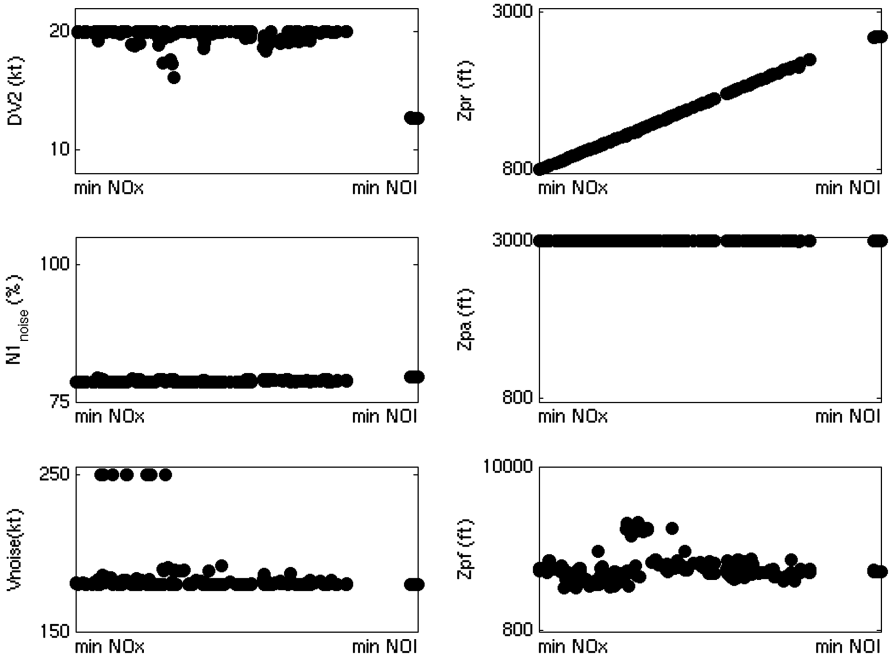

Fig. 13 Flight-path variables for the close-in noise–NOx BOP.

the protected area in order to maximize the rate of climb and, therefore, the distance to the microphone. However, once the protected zone has been passed, the speed profile can be adapted to reduce the other remaining criteria. Figure 10 shows that the optimum flight path is rather different in the cases where noise must be minimized in further zones. In these cases, the aircraft altitude before flying over the protected zone is higher than the maximum accepted thrust reduction altitude. Therefore, thrust is cut back at a high altitude near the maximum acceptable value, and it is not restored until the protected area has been flown over. An early acceleration allows the noise exposure time to be decreased over the protected area and the aircraft configuration to be changed sooner, so the aircraft speed has a major role.

The optimum levels of DOC and NOx are not dependant on the zone where noise is estimated, so the differences presented in Figs. 11 and 12 may be surprising. As mentioned previously, the mono-objective optimization problems of both criteria have multiple solutions. However, this multiplicity is removed when they are optimized together with another criterion.

In NOx optimization, a series of tradeoffs occur: an accelerated segment decreases the rate of climb, increasing the exposure time at low altitudes (negative effect on NOx emissions). However, flying at higher speeds permits climbing with higher rates of climb, which has a positive effect on NOx emissions. On the other hand, decreasing the cutback altitude also has two contradictory effects: the rate of climb is decreased (negative effect), but fuel flow is also decreased, which has a positive effect. During the optimization, there is a tradeoff between these four factors. Figure 11 shows that, among all these contradictory factors, the minimum NOx levels are achieved when the aircraft flies under the threshold altitude using the lowest possible engine rating (and so minimizing the combustion products). In these paths, the aircraft flies at the highest possible

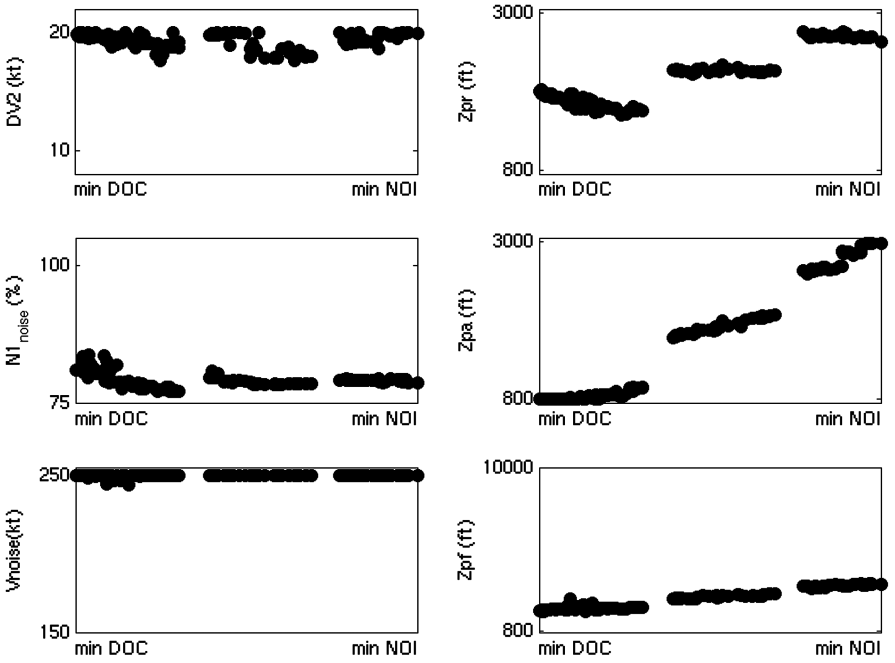

Fig. 14 Flight-path variables for the close-in noise–DOC BOP.

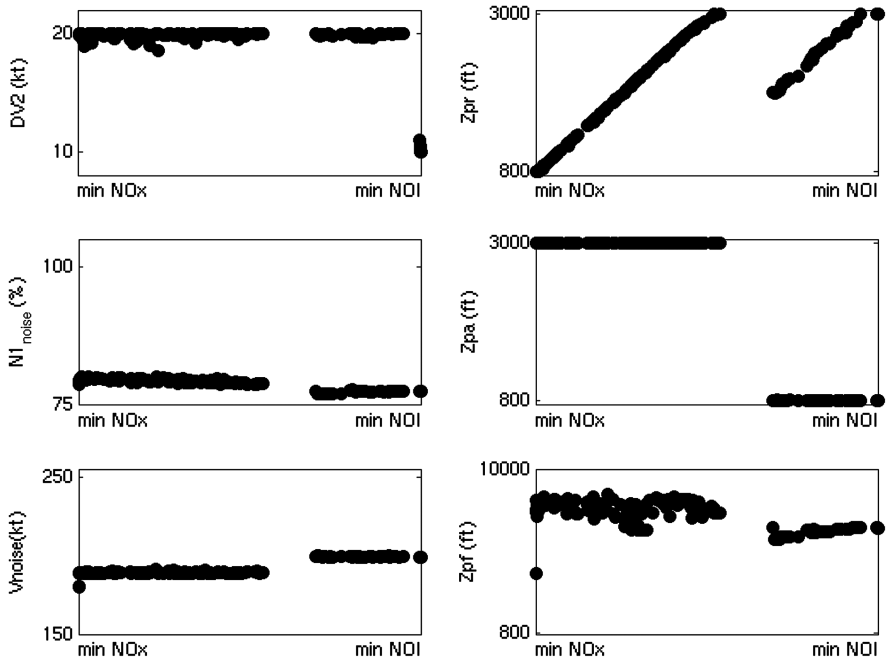

Fig. 15 Flight-path variables for the distant noise–NOx BOP.

rates of climb to decrease the exposure time at low altitude, so the acceleration segment starts after the threshold altitude has been reached. Then, once this threshold altitude has been reached, the flight path can be adapted to reduce other criteria. In scenario A, noise reduction mainly affects the flight paths at low altitudes too, so the departure procedure at higher altitudes is indeterminate. This means that, in this particular case, the extreme point of the Pareto front is not unique. Nevertheless, in the case of scenario B, thrust is restored further away from the airport to reduce the perceived noise in distant zones.

Another important result concerns the difference on the length of the segment at reduced thrust in the extreme solution of BOP-III [minimum distant noise protected zone (D-NOISE-III) and nitrogen oxides (NOx-III) flight paths]. The air quality criterion is insensitive to thrust restoration because it occurs at an altitude higher than the boundary altitude. Moreover, the noise generated by the aircraft impacts less and less of the protected zone area once it has been flown over, and so the length of the segment at the reduced engine rating does not affect the perceived noise in the protected zone anymore. Therefore, the length of the segment at thrust cutback is undetermined in this optimization problem. Finally, this means that optimum flight paths from Fig. 10 are similar, because they have been obtained using the same optimization algorithm.

Minimum operating cost paths are characterized by an early acceleration that permits the most efficient aircraft states to be reached earlier. The higher engine ratings should also be used, but they have a minor role, and thrust cutback can be adapted to reduce the perceived noise on the ground. Then, the minimum DOC flight path is not unique. For example, in Fig. 12, the DOC-II path consists of cutting back thrust earlier to ensure that the aircraft flies over the close-in zone at a reduced engine level.

This analysis of the guiding variables of the optimum flight paths corroborates the conclusions of Sec. VI.A. The general NADP 1 and NADP 2 can be optimized for minimum environmental impact.

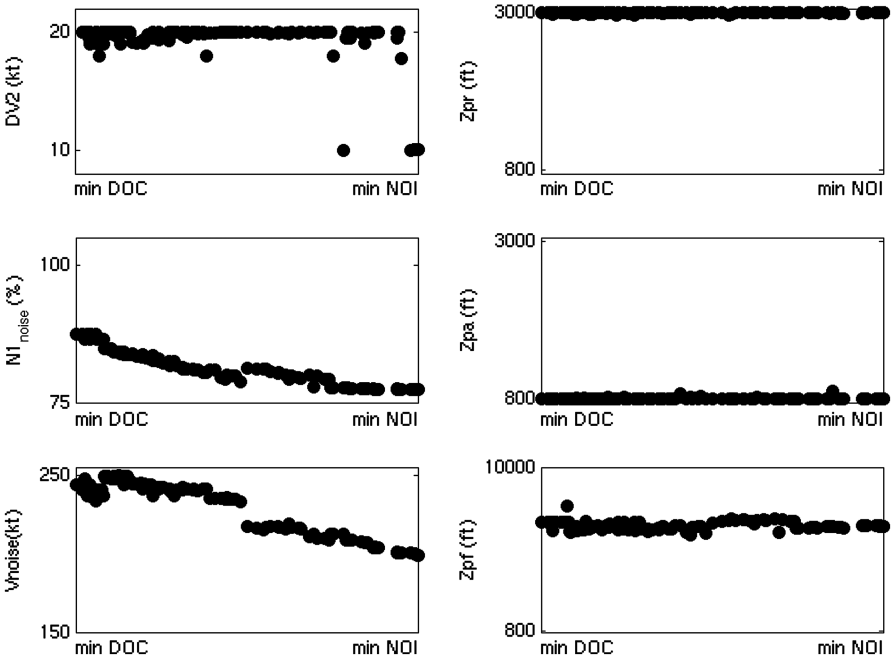

Fig. 16 Flight-path variables for the distant noise–DOC BOP.

C. Multicriteria Optimization: Evolution of Flight Paths Along the Pareto Front

In the previous sections, the characteristics of the extreme points of the Pareto fronts have been analyzed. This has enabled the optimization mechanisms of each environmental criterion to be analyzed. The main assets of the proposed method are in the ability to describe the intermediate solutions in the optimized environmental criteria. Using the conclusions of Sec. VI.B, it is possible to describe and understand the general shapes of the optimum fronts of Figs. 5–8 and the evolution of the optimum flight-path variables along them.

Figures 5–8 show that, in general, the Pareto fronts are not continuous. Indeed, these figures show that the noise criterion shows a continuous behavior, whereas small discontinuities can be seen in the cases of operating costs and nitrous oxides. This phenomenon is a direct consequence of the nonlinearity of the noise criteria. In the four optimization problems, the Pareto front is described by a series of optimum flight-path families (see Figs. 13–16). Each family is optimal in a restricted zone of the Pareto front. An extension of these families leads to either nonfeasible flight paths or to non-Pareto-optimal paths.

The sensitivity of each optimized variable is strongly influenced by the choice of BOP. Some of the optimum variables present oscillations along the Pareto fronts. This means that between the upper and lower oscillation bounds, the optimized criteria are insensitive to the selected variable. In other words, any intermediate value between the bounds is also optimal. In these cases, the evolutions of the flight-path variables can be smoothed to obtain regular or continuous behaviors.

In scenario A, the flight paths optimizing close-in noise and air quality only differ in the value of the cutback altitude (see Figs. 9–11), so only one family of optimal flight paths is obtained (see Fig. 13). In the minimum NOx path, engine rate is cut back as soon as possible to an optimized constant level. As the noise criterion becomes more important, the cutback altitude increases up to the altitude at which the aircraft flies over the protected zone. Finally, the aircraft target speed V_{noise} does not take very high values to remain at higher rates of climb. The thrust restoration altitude takes an oscillatory value. This means that it can take any value whenever it does not affect the perceived noise on the ground. These results are coherent with the ICAO recommendations to use these procedures to improve noise in zones close to airports.

On the contrary, the close-in noise–DOC front is obtained through several families of optimum procedures (see Fig. 14). Minimizing DOC is achieved through an E-NADP-2 type of procedure, characterized by an early acceleration, while minimum close-in noise flight paths allow the aircraft flying at higher altitudes, using lower engine ratings. Therefore, the optimization variables show a transition from minimum DOC to minimum noise flight paths. This transition is piecewise continuous, which means that optimization variables are clustered into families. Each family is characterized by a different pair of cutback and acceleration altitudes and an increasing thrust restoration altitude. It is also remarkable that the transition into two different families does not significantly change the level of noise. However, since the procedures are different, there are discontinuities in terms of fuel burn, which justifies the fact that the Pareto fronts are not continuous.

Similar to Figs. 13 and 14, several families of procedures define the optimum fronts in scenario B. The distant noise–NOx front is characterized by two families of procedures (Fig. 15). The first family, with a maximum acceleration altitude and an increasing cutback altitude, is very similar to the one seen in the close-in noise–NOx optimization problem, and it describes low air quality procedures, while the second family, an E-NADP-2 trajectory type with minimum acceleration altitude, defines the minimum distant noise zone of the Pareto front. In both families, the initial speed ΔV_2, the target speed V_{noise}, and the reduced engine rating levels take optimum, constant values.

Finally, the distant noise–DOC optimal front is constituted by E-NADP-2 (acceleration before thrust cutback). They are characterized by decreasing values of the target speed V_{noise} and the engine thrust and fixed values of the acceleration and thrust-cutback altitudes (see Fig. 16).

VII. Conclusions

This paper introduces a methodology for reducing the environmental footprint of aircraft based on the optimization of departure procedures. This concept has been formulated through a multiobjective, nonlinear, constrained optimization problem. To solve this problem efficiently, the recent multi-MADS method is proposed. This free derivative algorithm approximates the Pareto-optimal fronts by solving a series of single-objective optimizations using the MADS optimization method. The feasibility of this methodology is illustrated with a current in-production Airbus aircraft departing from an ideal airport. In this application, the three environmental criteria (noise, NOx emissions, and CO_2 emissions) have been optimized in pairs. The results of the problem are the optimal levels of the considered environmental criteria and their associated optimal flight paths. The study was performed in a research perspective using Airbus-designed office software. Keeping in mind that operational feasibility has not been confirmed, and the procedures have not been validated against Airbus standard operating procedures, these promising results still need an operational assessment.

Future related work will attempt to assess the validity of optimal departures in more advanced scenarios. For example, atmospheric conditions in a real operation may vary from the reference conditions assumed during the computation of the optimal procedures. Research will strive to obtain the maximum deviation from the reference atmospheric conditions, guaranteeing that the proposed flight paths remain nearly optimal.

Acknowledgments

This research was performed in Airbus Operations, S.A.S.. The authors would like to thank the Airbus Operations community, specializing in environmental subjects. Appreciation is also expressed to S. Digabel, from Ecole Politéchnique de Montreal, for his support on MADS utilization and his pertinent remarks on the first draft of the paper.

References

[1] Advisory Council for Aeronautics Research in Europe, "2008 Addendum to the Strategic Research Agenda," Brussels, 2008.

[2] International Civil Aircraft Organization, "Assembly Resolutions in force (as of 8 October 2004)," Doc. 9848, Montreal, 2004.

[3] International Civil Aircraft Organization, "Aircraft Operations. Volume I: Flight Procedures," Doc. 8168, Montreal, 2007.

[4] Clarke, J. P., and Hansman, R. J., Jr., "Parametric Study of the Noise Impact of Approach and Departure Maneuvers Using Advanced Flight Guidance Techniques," 33rd Aerospace Sciences Meeting and Exhibit, AIAA Paper 1995-0835, 1995.

[5] Clarke, J. P, "System Analysis of Noise Abatement Procedures Enabled by Advanced Flight Guidance Technology," *Journal of Aircraft*, Vol. 37, No. 2, March–April 2000, pp. 266–273. doi:10.2514/2.2590

[6] Visser, H. G., and Wijnen, R. A. A., "Optimization of Noise Abatement Departure Trajectories," *Journal of Aircraft*, Vol. 38, No. 4, July–Aug. 2001, pp. 620–627. doi:10.2514/2.2838

[7] Visser, H. G., and Wijnen, R. A. A., "Optimisation of Noise Abatement Arrival Trajectories," *The Aeronautical Journal*, Vol. 107, No. 1076, 2003, pp. 607–615.

[8] Hebly, S., and Visser, H. G., "Advanced Noise Abatement Departure Procedures: Custom Optimized Departure Profiles," Aircraft Technology, Integration and Operations Conference, AIAA Paper 2008-7405, Aug. 2008.

[9] Prats, X., Puig, V., Quevedo, J., and Nejjari, F., "Equitable Noise Abatement Departure Procedures," Aircraft Technology, Integration and Operations Conference, AIAA Paper 2009-6939, Sept. 2009.

[10] "Air Quality Procedures for Civilian Airports and Air Force Bases," Federal Aviation Administration, Rept. FAA-AEE-97-03 AL/EQ-TR-1996-0017, April 1997.

[11] International Civil Aircraft Organization (ICAO), "Airport Air Quality Guidance Manual," Doc. 9889, Montreal, 2007.

[12] Intergovernmental Panel on Climate Change, *Aviation and the Global Atmosphere*, Cambridge Univ. Press, Cambridge, England, U.K., 1999.
[13] Metz, B., Davidson, O., Bosch, P., Dave, R., and Meyer, L. (eds.), "Climate Change 2007: Mitigation of Climate Change," Cambridge Univ. Press, Cambridge, England, U. K., 2007.
[14] "Aviation and Climate Change," U. S. Government Accountability Office, Rept. GAO-09-554, June 2009, http://www.faa.gov/data_research/aviation/aerospace_forecasts/2009-2025/media/2009%20Forecast%20Doc.pdf [retrieved 27 Aug. 2010].
[15] "Environmental Review 2004," International Air Transportation Assoc., Montréal, Canada2004.
[16] "FAA Aerospace Forecast Fiscal Years 2009–2025," Federal Aviation Administration, 2009.
[17] "Global Market Forecast 2009–2028," Airbus, S.A.S., Toulouse, France, 2009.
[18] "PEP and LTS, Performance Engineers Program and Load and Trim Sheet Software," Airbus, S.A.S., Toulouse, France, 2003.
[19] DuBois, D., and Paynter, G. C., "Fuel Flow Method II for Estimating Aircraft Emissions," Society of Automotive Engineers TP 2006-01-1987, Warrendale, PA, Aug. 2006.
[20] "Getting to Grips with Cost Index," *Flight Operations Support and Line Assistance*, STL 9545.2369/96, No. II, Airbus, S.A.S., Toulouse, France, May 1998.
[21] Ehrgott, M., *Multicriteria Optimization*, Springer, Berlin, 2005.
[22] Audet, C., and Dennis, J. E. Jr., "Mesh Adaptive Direct Search Algorithms for Constrained Optimization," *SIAM Journal on Optimization*, Vol. 17, No. 1, 2006, pp. 188–217. doi:10.1137/040603371
[23] Le Digabel, S., "NOMAD: Nonsmooth Optimization with the MADS Algorithm," GERAD, TR G-2009-39, Montréal, Canada2009.
[24] Audet, C., Savard, G., and Zghal, W., "A Mesh Adaptive Direct Search Algorithm for Multi-Objective Optimization," *European Journal of Operational Research*, Vol. 204, No. 3, Aug. 2010, pp. 545–556. doi:10.1016/j.ejor.2009.11.010.
[25] Kolda, T., Lewis, R. M., and Torczon, V., "Optimization by Direct Search: New Perspectives on Some Classical and Modern Methods," *SIAM Review*, Vol. 45, No. 3, 2003, pp. 385–482. doi:10.1137/S003614450242889
[26] Audet, C., and Dennis, J. E., Jr., "A Progressive Barrier for Derivative Free Non-Linear Programming," *SIAM Journal on Optimization*, Vol. 20, No. 1, 2009, pp. 445–472. doi:10.1137/070692662
[27] "Review of Noise Abatement Procedure Research and Development and Implementation Results: Discussion of Survey Results," *CAEP: Committee on Aviation Environmental Protection, Working Group II*, International Civil Aviation Org., Montréal, Canada, April 2007.
[28] Audet, C., Savard, G., and Zghal, W., "Multiobjective Optimization Through a Series of Single Objective Formulations," *SIAM Journal on Optimization*, Vol. 19, No. 1, 2008, pp. 188–210. doi:10.1137/060677513